# $^{57}$Fe Mössbauer study of $ATiRO_5$ compounds ($A$ = Cr, Mn, Fe, and $R$ = Pr, Nd, Sm, Eu, Gd)

P. J. Schurer and A. H. Morrish
*Department of Physics, University of Manitoba, Winnipeg, Manitoba, Canada R3T 2N2*
(Received 22 February 1977)

The results of an $^{57}$Fe Mössbauer study of $ATiRO_5$ compounds at 4.2 and 295 K are interpreted on the basis of covalency contributions to the isomer shift and magnetic hyperfine fields. Above 4.2 K relaxation effects are observed in the Mössbauer spectra.

## I. INTRODUCTION

The compounds $ATiRO_5$ ($A$ = Cr, Mn, Fe and $R$ = Pr, Nd, Sm, Eu, Gd) belong to the orthorhombic space group *Pbam* and are antiferromagnets at low temperatures. The $A^{3+}$ and $Ti^{4+}$ ions occupy the $4f$ and $4h$ sites in this space group which have octahedral and square-pyramidal oxygen environments, respectively. A neutron-diffraction study of the Nd compounds showed that the $Cr^{3+}$ ions have a strong preference for the octahedral site, whereas the $Fe^{3+}$ and $Ti^{4+}$ ions are almost equally distributed over the $4f$ and $4h$ sites. The $Nd^{3+}$ ions occupy the $4g$ positions. No experimental information on the distribution of $Mn^{3+}$ and $Ti^{4+}$ in the Mn compounds is available.[1]

Previously, the results of Mössbauer-effect (ME) measurements at 4.2 K on compounds with $R$ = Nd have been reported,[2] and were in fair agreement with the neutron-diffraction measurements. It is of interest to attempt a more systematic study of the compounds. A change in the rare-earth ion at the $4g$ site may cause a systematic variation in some of the properties of the $3d$ transition ions on the $4f$ and $4h$ sites. Consequently, important information on the correlation between these properties can be obtained.

## II. EXPERIMENTAL

The compounds $FeTiRO_5$ (with iron 20% enriched in $^{57}$Fe), $Mn_{0.95}Fe_{0.05}TiRO_5$, and $Cr_{0.95}Fe_{0.05}TiRO_5$ (both 70% enriched) have been prepared in a way similar to that described by Buisson.[1] A stoichiometric mixture of powders was pressed into a pellet and fired at 1225 °C in a platinum crucible for 48 h in air. If necessary, the sample was reground and the procedure repeated. X-ray diffraction and ME measurements showed that the total amount of impurity phases containing iron, was less than ~1% for all samples with the possible exception of $Cr_{0.95}Fe_{0.05}TiNdO_5$.

X-ray diffractograms of the compounds have been obtained using Cu ($K\alpha$) radiation. The crystal-lattice parameters have been determined from a least-squares fit of the $d_{hkl}$ values. The results (Table I) are in good agreement with those reported before.[1] By using the atomic position parameters, the $A^{3+}$-$O^{2-}$ distances for the octahedral and the square pyramidal sites in $FeTiNdO_5$ and $CrTiNdO_5$ have been calculated (Table II). The octahedrons in both compounds are distorted by a compression along one of the axes. The compression is 7% for $FeTiNdO_5$ and 11% for $CrTiNdO_5$.

The ME measurements have been performed with an Elscint spectrometer which produces linewidths of 0.28 mm/sec for the outer lines of a natural iron calibration absorber 10 $\mu$m thick. The measurements below room temperature were performed in a variable temperature cryostat (Oxford Instruments) which has a temperature stability of 0.1 K. The amount of $^{57}$Fe in the absorbers was ~0.4 mg/cm$^2$ for the $FeTiRO_5$ compounds and ~0.2 mg/cm$^2$ for the other two series.

The shape of the ME spectra at room temperature depends mainly on the kind of $A^{3+}$ ion and,

TABLE I. Lattice parameters of $ATiRO_5$ (Å).

| | $Cr_{0.95}Fe_{0.05}TiRO_5$ | | | $Mn_{0.95}Fe_{0.05}TiRO_5$ | | | $FeTiRO_5$ | | |
|---|---|---|---|---|---|---|---|---|---|
| | $a$ | $b$ | $c$ | $a$ | $b$ | $c$ | $a$ | $b$ | $c$ |
| Pr | 7.61 | 8.69 | 5.81 | 7.60 | 8.73 | 5.84 | 7.60 | 8.74 | 5.85 |
| Nd | 7.58 | 8.68 | 5.81 | 7.56 | 8.71 | 5.83 | 7.57 | 8.72 | 5.84 |
| Sm | 7.51 | 8.62 | 5.79 | 7.49 | 8.65 | 5.81 | 7.50 | 8.68 | 5.83 |
| Eu | 7.47 | 8.60 | 5.78 | 7.46 | 8.62 | 5.81 | 7.47 | 8.66 | 5.83 |
| Gd | 7.45 | 8.59 | 5.79 | 7.46 | 8.58 | 5.80 | 7.44 | 8.65 | 5.83 |

TABLE II $A^{3+}$ cation–oxygen distance (Å).

| Site | Bond | $CrTiNdO_5$ | $FeTiNdO_5$ |
|---|---|---|---|
| Square-Pyramid (4*h*) | $A^{3+}$-$O_{(1)}$ | 1.80 | 1.84 |
| | $A^{3+}$-$O_{(2,3)}$ | 1.89 | 1.92 |
| | $A^{3+}$-$O_{(4,5)}$ | 1.92 | 1.97 |
| | Average | 1.88 | 1.92 |
| Octahedron (4*f*) | $A^{3+}$-$O_{(1,2)}$ | 1.93 | 1.96 |
| | $A^{3+}$-$O_{(3,4)}$ | 2.05 | 2.18 |
| | $A^{3+}$-$O_{(5,6)}$ | 2.11 | 2.21 |
| | Average | 2.03 | 2.11 |

for the same $A^{3+}$ ion, is not affected much by the choice of $R^{3+}$ ion. For this reason the three series $FeTiRO_5$, $Mn_{0.95}Fe_{0.05}TiRO_5$, and $Cr_{0.95}Fe_{0.05}TiRO_5$ will be discussed separately. Relaxation phenomena, observed for a range of temperatures well below $T_N$, are discussed at the end.

## III. RESULTS AND DISCUSSION

### A. $FeTiRO_5$ compounds ($R$ = Pr,Nd,Sm,Eu,Gd)

In Fig. 1, the ME spectra of two members in this series are shown for room temperature and $T$ = 4.2 K. The spectra at room temperature consist of two broadened absorption peaks, slightly different in depth. A computer fit with one quadrupole split pattern gives an isomer shift of $\delta$ = 0.3 mm/sec relative to metallic iron. This value is in good agreement with that expected for $Fe^{3+}$ ions. The linewidth is $\Gamma \approx 0.61$ mm/sec. The six-line spectra at 4.2 K are also asymmetric with linewidths $\Gamma \approx 1.3$ mm/sec. The broad linewidths, together with the asymmetry in the depth of the absorption lines indicate that $Fe^{3+}$ ions are located at both the 4*f* and 4*h* sites in these compounds. As a result the spectra consist of two components because the quadrupole splitting $\epsilon$, the isomer shift $\delta$, and the magnetic hyperfine field $H_{hf}$, at $^{57}Fe$ nuclei are different for $Fe^{3+}$ ions at 4*f* and 4*h* sites. In order to identify the two components in the ME spectra it is useful to discuss these three quantities.

The quadrupole splitting results from the interaction between the nuclear-quadrupole moment $Q$ and the electric field gradient (EFG) at the $^{57}Fe$ nucleus, viz.,

$$\epsilon = \tfrac{1}{2}e^2qQ(1+\tfrac{1}{3}\eta^2)^{1/2} ,$$

where

$$\eta = (V_{xx} - V_{yy})/V_{zz}$$

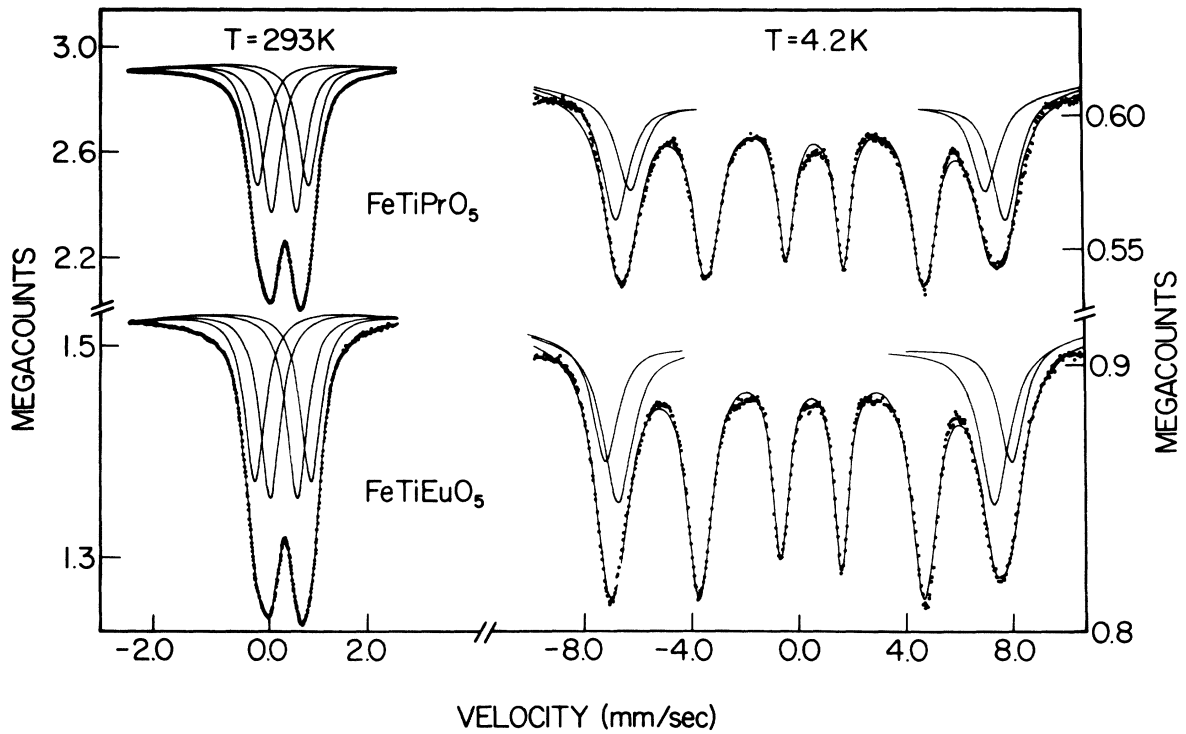


FIG. 1. Mössbauer spectra of $FeTiPrO_5$ and $FeTiEuO_5$ at 293 and 4.2 K. The points represent the experimental data and the curves the two individual patterns and their sum as obtained by a computer fit.

and

$$eq = V_{zz} = (1-\gamma_\infty)V_{zz}^{\text{latt}} + (1-\mathcal{R})V_{zz}^{\text{ion}} .$$

Here $V_{zz}^{\text{latt}}$ is the contribution to the EFG from the surrounding ions, whereas $V_{zz}^{\text{ion}}$ is that from electrons of the ion itself. The effects of shielding and antishielding of the nucleus by the core electrons is represented by $\mathcal{R}$ and $\gamma_\infty$, respectively.

For $Fe^{3+}$ ions, $V_{zz}^{\text{ion}}$ is determined by the amount of overlap distortion of the closed-shell $Fe^{3+}$ orbitals by ligand orbitals and by the amount of charge transfer from ligand to empty $Fe^{3+}$ orbitals. However, it is estimated that the $V_{zz}^{\text{ion}}$ contribution to $V_{zz}$ is only of the order of 20%.[3] For this reason, since we are only interested in the difference between $V_{zz}(4h)$ and $V_{zz}(4f)$, we have assumed $V_{zz} = (1-\gamma_\infty)V_{zz}^{\text{latt}}$.

From the point-ion model,

$$V_{zz}^{\text{latt}} = \sum_i \frac{3\cos^2\theta_i - 1}{r_i^3} e_i ;$$

$V_{zz}^{\text{latt}}$ is calculated by summing the contributions from charges $e_i$ of ions at positions $(r_i, \theta_i)$ inside a sphere of 60 Å. Values of $\gamma_\infty = -7.97$ determined by Gupta and Sen,[4] and $Q = 0.2$ barns have been used. The results depend strongly on the distribution of $A^{3+}$ and $Ti^{4+}$ ions over the $4f$ and $4h$ sites.

Neutron-diffraction measurements[1] show that the $Fe^{3+}$ and $Ti^{4+}$ ions are almost equally distributed over the $4f$ and $4h$ sites. Therefore, in order to get a realistic distribution of charges for the calculation of $V_{zz}^{\text{latt}}$, 3+ and 4+ charges were generated at random at $4f$ and $4h$ sites inside the sphere at 60 Å. This radius was considered to be sufficiently large since the results for a 50-Å sphere differed by only 5%. Mean values $\bar{\epsilon}(4h)$ and $\bar{\epsilon}(4f)$, and standard deviations were determined by calculating the EFG ten times for each site. The results are $\bar{\epsilon}(4h) = 0.78 \pm 0.08$ mm/sec and $\bar{\epsilon}(4f) = 1.43 \pm 0.19$ mm/sec. From the standard-deviation values, the distribution is expected to produce ~20% line broadening.

Not only $\epsilon$ but also $\delta$ and $H_{\text{hf}}$ are expected to be different for $Fe^{3+}$ at $4f$ and $4h$ sites. It is well known that the differences in $\delta$ and $H_{\text{hf}}$ measured for $Fe^{3+}$ in various oxygen surroundings (octahedral, tetrahedral, etc.) can be understood by overlap-distortion and charge-transfer effects,[3,5-9] that is

$$\delta = \delta_{\text{free}} + \delta_{\text{cov}} + \delta_{\text{red}}$$

and

$$H_{\text{hf}} = H_{\text{free}} + H_{\text{cov}} + H_{\text{red}} + H_{\text{st hf}} .$$

The origin of $\delta_{\text{cov}}$ and $H_{\text{cov}}$ lies in the overlap of doubly occupied $Fe^{3+}$ $ns$ orbitals with oxygen $p$ orbitals and in the transfer of $p$ electrons into empty $4s$ orbitals. In a similar way, the source of $\delta_{\text{red}}$ is in the overlap and transfer effects involving the $3d$ orbitals of the $Fe^{3+}$ ion. Finally, the supertransferred hyperfine field $H_{\text{st hf}}$ is produced by the transfer of $p$ electrons into empty $3d$ orbitals of neighboring magnetic ions in the superexchange bond.

In the notation of Sawatzky *et al.*,[3,7-9] the various contributions can be calculated from the following relationships:

$$H_{\text{free}} = -630 \text{ kOe},$$

$$\delta_{\text{cov}} = -p[\tfrac{1}{2}(N^{\uparrow 2} + N^{\downarrow 2})](\alpha^{\downarrow 2} + \alpha^{\downarrow 2})\,0.14 \quad (\text{mm/sec}),$$

$$H_{\text{cov}} = 525p[\tfrac{1}{2}(N^{\uparrow 2} + N^{\downarrow 2})](\alpha^{\uparrow 2} - \alpha^{\downarrow 2}) \quad (\text{kOe}),$$

$$\delta_{\text{red}} = p[(N_\sigma^\uparrow S_\sigma^\uparrow)^2 + (N_\sigma^\downarrow B_\sigma^\downarrow)^2]0.25 \quad (\text{mm/sec}),$$

$$H_{\text{red}} = -\tfrac{630}{5}p[(N_\sigma^\uparrow S_\sigma^\uparrow)^2 - (N_\sigma^\downarrow B_\sigma^\downarrow)^2] \quad (\text{kOe}),$$

$$H_{\text{st hf}} = -\tfrac{525}{2} N^{\uparrow\downarrow}(\alpha^{\uparrow 2} + \alpha^{\downarrow 2})]\langle\cos^2\theta\rangle_{\text{av}} \times \sum_{i=1}^{m} (B_{\sigma i}^{nn} + S_{\sigma i}^{nn})^2 \quad (\text{kOe}),$$

where

$$N^{\uparrow\downarrow 2} = (1 + S_{zz} - p\sum_n S_{ns}^{\uparrow\downarrow 2} + pa_{4s}'^2 + 2pa_{4s}'S_{4s}')$$

$$a^{\uparrow\downarrow} = -\sum_n S_{ns}^{\uparrow\downarrow}\phi_{ns}^{\uparrow\downarrow}(0) + a_{4s}'\phi_{4s}^{\uparrow\downarrow}(0) .$$

Here $p = 5$ or 6 for a $4h$ or $4f$ site, respectively, and $m$ is the total number of nearest-neighbor $Fe^{3+}$ ions. The values of the single-orbital overlap integrals $S_{ns}' = \langle p|\phi_{ns}\rangle$ and $S_\sigma = \langle p^\uparrow | d_{3z^2-r^2}^\uparrow\rangle$ have been reported by Sawatzky *et al.*[8] for various $Fe^{3+}$-$O^{2-}$ distances. A value of $S_{zz} = 0.23678$ for the ligand-ligand integral was employed.[9] For octahedral sites transfer integral values of $a_{4s}'(p_z \rightarrow \phi_4) = 0.125$ and $B_\sigma(p_z^\downarrow \rightarrow d_{3z^2-r^2}^\downarrow) = 0.320$ have been found experimentally for a $Fe^{3+}$-$O^{2-}$ distance of 2.011 Å.[9] If $B_\sigma \propto S_\sigma$ and $a_{4s}' \propto S_{4s}'$ then for an average $Fe^{3+}$-$O^{2-}$ distance of 2.11 Å (Table II) values of $B_\sigma(4f) = 0.286$ and $a_{4s}'(4f) = 0.121$ are reasonable to use in the calculation. By the same arguments $a_{4s}'(4h) = 0.181$ and $B_\sigma(4h) = 0.466$ have been used. The results are shown in Table III.

From the calculations for $\epsilon$, $\delta$, and $H_{\text{hf}}$ the conclusion is drawn that ME spectra should be fitted with two absorption patterns, the one with the largest values of $\epsilon$, $\delta$, and $H_{\text{hf}}$ corresponding to

TABLE III. Covalency contributions to the isomer shift $\delta$ (mm/sec) and the magnetic hyperfine field $H_{\text{hf}}(0)$ (kOe) for $FeTiNdO_5$.

| Site | $\delta_{\text{cov}}$ | $\delta_{\text{red}}$ | $H_{\text{cov}}$ | $H_{\text{red}}$ | $\bar{H}_{\text{st hf}}$ | $H_{\text{hf}}(0)$ |
|---|---|---|---|---|---|---|
| $4f$ | −0.606 | 0.096 | 73 | 43 | −22 | −536 |
| $4h$ | −0.875 | 0.169 | 111 | 79 | −8 | −448 |

TABLE IV. Experimental values of the linewidth $\Gamma$ (mm/sec); the isomer shift, relative to metallic iron, $\delta$ (mm/sec); the quadrupole splitting $\epsilon$ (mm/sec); and the $Fe^{3+}$ distribution over $4f$ and $4h$ sites (%), in $A\,Ti\,RO_5$ compounds from least-squares fits of Mössbauer spectra measured at room temperature. The figures in parentheses are the probable errors.

| | $R$ | $\Gamma$ | $\delta(4h)$ | $\epsilon(4h)$ | $\delta(4f)$ | $\epsilon(4f)$ | $Fe^{3+}$ at $4h$ |
|---|---|---|---|---|---|---|---|
| $FeTiRO_5$ | Pr | 0.43 | 0.34(1) | 0.47(1) | 0.33(1) | 0.95(1) | 55(5) |
| | Nd | 0.39 | 0.34 | 0.51 | 0.33 | 0.92 | 60 |
| | Sm | 0.45 | 0.32 | 0.49 | 0.31 | 1.00 | 55 |
| | Eu | 0.45 | 0.32 | 0.49 | 0.31 | 1.03 | 50 |
| | Gd | 0.46 | 0.33 | 0.50 | 0.31 | 1.05 | 50 |
| | average | 0.44 | 0.33 | 0.49 | 0.32 | 0.99 | 55 |
| $Mn_{0.95}Fe_{0.05}TiRO_5$ | Pr | 0.36 | 0.31 | 0.89 | 0.33 | 0.54 | 50 |
| | Nd | 0.38 | 0.30 | 0.91 | 0.33 | 0.55 | 55 |
| | Sm | 0.35 | 0.30 | 0.94 | 0.33 | 0.59 | 55 |
| | Eu | 0.36 | 0.30 | 0.95 | 0.33 | 0.62 | 50 |
| | Gd | 0.34 | 0.31 | 0.96 | 0.33 | 0.63 | 45 |
| | average | 0.36 | 0.30 | 0.93 | 0.33 | 0.59 | 50 |
| $Cr_{0.95}Fe_{0.05}TiRO_5$ | Pr | 0.46 | 0.31 | 0.66 | 0.35 | 0.20 | 75 |
| | Nd | 0.47 | 0.31 | 0.68 | 0.37 | 0.24 | 75 |
| | Sm | 0.47 | 0.30 | 0.65 | 0.37 | 0.20 | 80 |
| | Eu | 0.49 | 0.30 | 0.68 | 0.36 | 0.23 | 80 |
| | Gd | 0.49 | 0.30 | 0.64 | 0.37 | 0.21 | 80 |
| | average | 0.48 | 0.30 | 0.66 | 0.36 | 0.21 | 80 |

$Fe^{3+}$ ions at $4f$ sites, and the other to $Fe^{3+}$ ions at $4h$ sites.

The spectra at room temperature have been fitted with two quadrupole-split absorption patterns using Lorentzian line shapes. The large overlap made it necessary to constrain the linewidths of the two patterns to be equal. The results are shown in Table IV. The values of $\epsilon$ and $\delta$ and the distribution of $Fe^{3+}$ ions are essentially the same for all five compounds. However, a slight increase in $\epsilon$ and possibly a slight decrease in $\delta$ is observed going from the Pr to the Gd compound in this series. As shown in Fig. 2, the values of $\epsilon$ are independent of temperature.

In Table V the results of computer fits to the spectra at 4.2 K using two six-line absorption patterns are presented. Here no constraint between the linewidths of the two patterns was imposed. Probably this is the reason why the intensities of the $4f$ and $4h$ patterns are slightly different from those of the spectra at room temperature. However, both measurements show that the $Fe^{3+}$ and therefore also the $Ti^{4+}$ ions are approximately equally distributed over the $4f$ and $4h$ sites. The decrease in $\delta(4f)$ and $\delta(4h)$ going from Pr to Gd is more pronounced in the experimental results obtained at 4.2 K. Furthermore the values of $H_{hf}$ change significantly with a rare-earth ion. The Néel temperatures $T_N$ determined by the onset of hyperfine splitting, also depend on the rare-earth ion. The hyperfine fields for $FeTiRO_5$ determined at $T = 0.08T_N$ are also listed in Table V in order to provide a more meaningful comparison between the different compounds in the series.

The values of $\delta_{cov}$, $\delta_{red}$, $H_{cov}$, $H_{red}$, $H_{st\,hf}$, and the Néel temperature $T_N$, depend on the Fe-O distances. $T_N$ and $H_{st\,hf}$ depend furthermore on the superexchange bond angle $\theta$.[7] It should be possible therefore to relate changes in $\delta$, $H_{hf}$, $T_N$, and also $\epsilon$ with changes in the Fe-O distances and in the angles $\theta$ for this series of compounds. The lattice parameters $a$, $b$, $c$ of the orthorhombic unit cell decrease by approximately 2%, 1%, and 0.05%, respectively, in going from Pr to Gd. This result appears to indicate that the Fe-O distance decreases. On the other hand, the atomic position parameters and, as a result, the superexchange bond angles may also have changed. The position parameters have only been measured for the $FeTiNdO_5$ compound. Therefore, the behavior of the Fe-O distances and angles $\theta$ is not known going from Pr to Gd in this series.

The decrease in $\delta$ and the increase in $\epsilon$ are consistent with a decreasing Fe-O distance alone. Then, a decrease in $H_{hf}$ but an increase of $T_N$ are also expected. However, $H_{hf}$ and $T_N$ first increase between Pr and Sm, and then decrease slightly between Sm and Gd. Since both $H_{st\,hf}$ and $T_N$ are linearly proportional to $\langle\cos^2\theta\rangle_{av}$,[9] these results can possibly be explained by a change in the superchange bond angle.

The experimental difference between $H_{hf}(4f)$ and

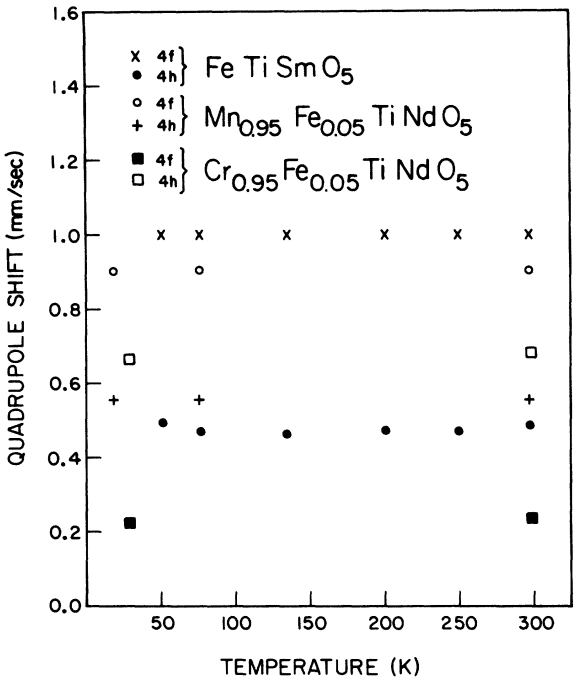


FIG. 2. Temperature dependence of the quadrupole splittings of the $4f$ and $4h$ absorption patterns measured for FeTiSmO$_5$, Mn$_{0.95}$Fe$_{0.05}$TiNdO$_5$, and Cr$_{0.95}$Fe$_{0.05}$ TiNdO$_5$.

$H_{hf}(4h)$ and also between $\delta(4f)$ and $\delta(4h)$ are smaller than expected from the calculation (Table III). The reason probably lies in inadequate assumptions made in the calculation. For instance, the calculation does not include the effects of overlapping orbitals of neighboring $A^{3+}$ ions at the $4f$ sites which are only separated by about 2.9 Å from each other.

### B. Mn$_{0.95}$Fe$_{0.05}$Ti$R$O$_5$

For this series of compounds the special position parameters for the atomic positions are not known and furthermore no experimental information about the distribution of $Mn^{3+}$ and $Ti^{4+}$ ions over the $4f$ and $4h$ sites is available. By comparing the crystal-field stabilization energies for $Mn^{3+}$ at octahedral and square-pyramidal sites, Buisson[1] argued that the $Mn^{3+}$ ions are expected to prefer the $4h$ site. With the assumption that all the $Ti^{4+}$ ions occupy the $4f$ sites and all the $A^{3+}$ ions occupy the $4h$ sites, the quadrupole splittings can be calculated using the special position parameters of either the CrTiNdO$_5$ or the FeTiNdO$_5$ compounds. However, the results are quite different. Hence, without the knowledge of the atomic position parameters, the EFG calculations probably cannot be used for the analysis of the ME spectra at room temperature.

As for the FeTi$R$O$_5$ compounds, the asymmetrical shapes of the spectra, illustrated in Fig. 3, indicate that $Fe^{3+}$ ions are present on both the $4f$ and $4h$ sites, and the spectra have therefore been fitted with two absorption patterns. The results are shown in Tables IV and V. The pattern with the largest value of $\delta$ and $H_{hf}$ have been identified with the $4f$ site. The quadrupole splitting is independent of the temperature (Fig. 2). The uncertainty in the parameters obtained for the spectra at 4.2 K is large because the overlap of the two patterns is large.

The behavior of $\epsilon$, $\delta$, and $H_{hf}$ in going from Pr to Gd in this series of compounds is similar to that found for the FeTi$R$O$_5$ compounds and therefore probably has the same origin. The values of $T_N$ are not significantly different for the five compounds.

For $Fe^{3+}$ and $Ti^{4+}$ ions the crystal-field stabiliz-

TABLE V. Experimental values of the isomer shift $\delta$ (mm/sec) relative to metallic Fe, the magnetic hyperfine field $H_{hf}$ (kOe), the Néel temperature $T_N$ (K), and the $Fe^{3+}$ distribution over $4f$ and $4h$ sites (%) in $A$TiRO$_5$ compounds from least-squares fits of Mössbauer spectra at 4.2 K. Also listed are the hyperfine fields (kOe) for FeTi$R$O$_5$ for the temperature $T=0.08T_N$ (K). The figures in parentheses are the probable errors.

| | | | | $T$ = 4.2 K | | | | $T=0.08T_N$ | |
|---|---|---|---|---|---|---|---|---|---|
| | $R$ | $T_N$ | $Fe^{3+}$ at $4h$ | $\delta(4h)$ | $\delta(4f)$ | $H_{hf}(4h)$ | $H_{hf}(4f)$ | $H_{hf}(4h)$ | $H_{hf}(4f)$ |
| FeTi$R$O$_5$ | Pr | 38.3(3) | 40(5) | 0.40(1) | 0.43(1) | 413(2) | 452(2) | 417(2) | 455(2) |
| | Nd | 33.5 | 50 | 0.40 | 0.42 | 432 | 465 | 436 | 469 |
| | Sm | 52.8 | 55 | 0.39 | 0.43 | 442 | 476 | 442 | 476 |
| | Eu | 52.0 | 60 | 0.39 | 0.40 | 430 | 465 | 430 | 465 |
| | Gd | 49.5 | 60 | 0.37 | 0.38 | 427 | 460 | 427 | 460 |
| Mn$_{0.95}$Fe$_{0.05}$Ti$R$O$_5$ | Pr | 19(1) | 35(5) | 0.42(2) | 0.43(2) | 404(4) | 449(4) | | |
| | Nd | 16 | 35 | 0.45 | 0.43 | 379 | 435 | | |
| | Sm | 19 | 45 | 0.41 | 0.41 | 415 | 456 | | |
| | Eu | 17 | 45 | 0.40 | 0.40 | 419 | 461 | | |
| | Gd | 18 | 40 | 0.36 | 0.38 | 414 | 458 | | |

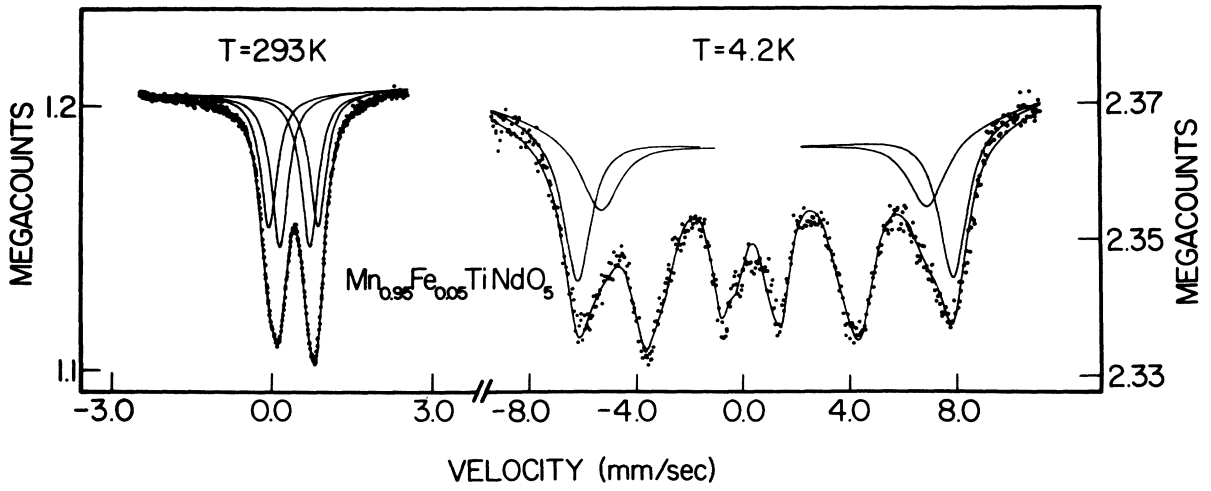


FIG. 3. Mössbauer spectra of $Mn_{0.95}Fe_{0.05}TiNdO_5$ at 293 and 4.5 K.

ation energy is zero for both the $4f$ and $4h$ sites. Therefore, the $Fe^{3+}$ and $Ti^{4+}$ ions have no preference for either site and, as observed, this leads to approximately equal intensities for the two $4h$ and $4f$ absorption patterns in the $FeTiRO_5$ spectra. On the other hand, the stabilization energies of the $Mn^{3+}$ ions are $-9.14Dq$ for the $4h$ and $-6Dq$ for the $4f$ sites.[10] Here $Dq$ is the octahedral-splitting parameter. Consequently, the $Mn^{3+}$ ions are expected to prefer the $4h$ site. The $4f$ absorption pattern is then expected to have the largest intensity. In reality, however, the ME spectra show that the $Mn^{3+}$ ions have only a slight preference for the $4h$ site at 4.2 K and none at all at room temperature. Apparently the difference in stabilization energy between the $4f$ and $4h$ sites is smaller than expected; the cause could be one or both of the following effects.

In a compression along the $z$ axis the $d_{x^2-y^2}$ energy level is lowered. Hence, the stabilization energy of an $Mn^{3+}$ ion in the octahedron will become more negative and the difference in stabilization between $Mn^{3+}$ at $4f$ and $4h$ sites will be decreases. In addition this difference will decrease even more if covalent transfer increases the number of electrons in the $3d$ orbitals of $Mn^{3+}$.

### C. $Cr_{0.95}Fe_{0.05}TiRO_5$

Neutron-diffraction measurements have shown that for the $CrTiNdO_5$ compound the most probable distribution of $Cr^{3+}$ ions over the two available lattice sites is 95% at $4f$ and 5% at $4h$ sites.[1] We assume that this distribution is not altered much when $Fe^{3+}$ replaces 5% of the $Cr^{3+}$ ions and that the $Fe^{3+}$ and $Ti^{4+}$ ions do not have a preference for either site. Then, about 90% of the $Fe^{3+}$ ions will occupy the $4h$ site and the other 10% the $4f$ site. For simplicity, the EFG at $^{57}Fe$ nuclei for the two sites has been calculated assuming that all the $A^{3+}$ ions are at $4f$ sites and all the $Ti^{4+}$ ions are at $4h$ sites. Then values of $\epsilon(4h) = 0.51$ mm/sec and $\epsilon(4f) = 0.25$ mm/sec are obtained. As a consequence the spectra at room temperature have been fitted with two absorption patterns; the one with the largest $\epsilon$ has been associated with the $4h$ site (Table IV). A room-temperature spectrum together with a computer fit is shown in Fig. 4. In this series of compounds the values of $\delta$ and $\epsilon$ do not change significantly, going from Pr to Gd. Furthermore, $\epsilon$ is independent of temperature (Fig. 2).

From the neutron-diffraction measurements it was found that in $CrTiNdO_5$ the spins at both the Cr and Nd ions become ordered below 13 K. The transition temperature $T_N = 17$ K found from ME measurements for $Cr_{0.95}Fe_{0.05}TiNdO_5$ is close to this value. The values of $T_N$ using the ME technique for the other compounds are quite different. For the Sm compound $T_N = 11$ K and the spectra at 4.2 K shows a hyperfine-split spectrum with very broad lines.

The spectrum at 4.2 K for the Eu sample is a broadened quadrupole-split spectrum. The broadening disappears at $T = 5.6$ K. The spectra of both the Pr and Gd sample at 4.2 K possess quadrupole splitting with no broadening; they start to broaden on reducing the temperature to about 3 K.

The ME spectrum of $Cr_{0.95}Fe_{0.05}TiNdO_5$ at 4.2 K has clearly two components as shown in Fig. 4. The largest (95%) can be associated with $4h$ sites and the smallest either with $4f$ sites or with an impurity phase. If the first possibility is true the values obtained from a fit of the spectrum are

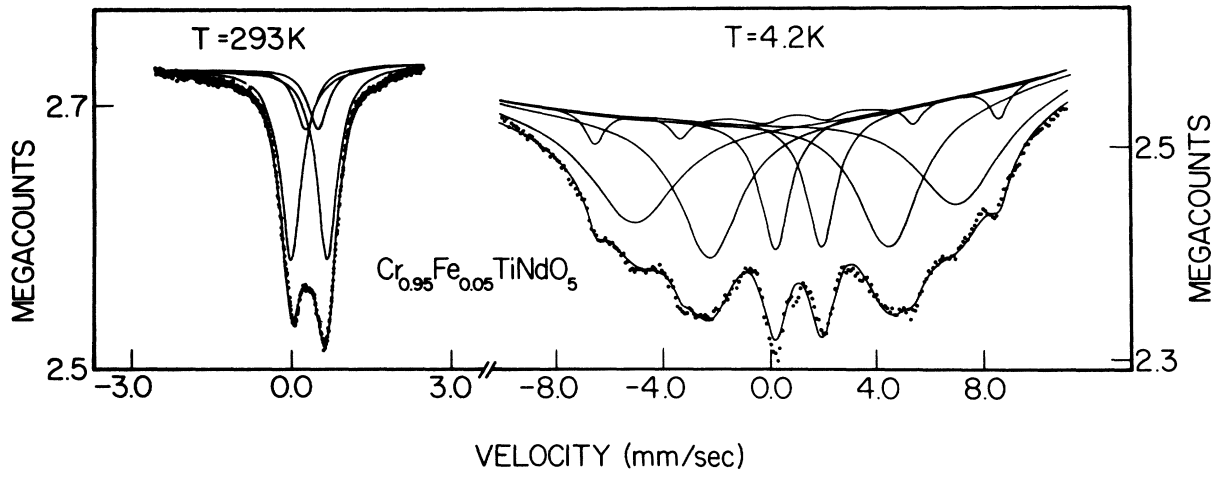


FIG. 4. Mössbauer spectra of $Cr_{0.95}Fe_{0.05}TiNdO_5$ at 293 and 4.5 K.

$H_{hf}(4f) = 466(1)$ kOe, $H_{hf}(4h) = 381(3)$ kOe, $\delta(4f) = 0.40(1)$ mm/sec, and $\delta(4h) = 0.41(1)$ mm/sec. None of the other compounds show the presence of a small intensity hyperfine-split component. Furthermore, this component is not present above the Néel temperature of $T_N = 17$ K. The possible impurity compounds are therefore considerably limited. For instance the compounds $FeNdO_3$, $CrNdO_3$, $Fe_2O_3$, and $Cr_2O_3$ which, according to the phase diagram, are most likely to be present as impurities,[1] have much higher $T_N$ values. Nevertheless, the presence of a 5% impurity phase cannot be completely excluded, since the absorption lines of the large component are about four times wider than those of the small component. For the large component the linewidths of corresponding pairs were allowed to vary independently. The outer lines are much broader than the inner ones. Either a distribution of hyperfine fields or relaxation effects could be the source of this observation.

### D. Relaxation effects

At temperatures above 4.2 K, the ME spectra show relaxation features at values of $T/T_N \ll 1$, as illustrated for $FeTiSmO_5$ in Fig. 5. The outer lines broaden considerably with increasing temperature and the intensity of the inner lines increase at the expense of the outer lines. The hyperfine fields at the two sites have temperature dependences that are not significantly different. For this reason, their average $\bar{H}_{hf}(T)/H_{hf}(0)$, has been reproduced in Fig. 6. A comparison with a Brillouin curve calculated for $S = \frac{5}{2}$ shows that an appreciable difference exists. For spectra taken at temperatures between $0.7 < T/T_N < 1$ the coexistence of a paramagnetic component and a broadened Zeeman-split component is observed.

Relaxation effects in ME spectra have been discussed by various authors.[11-14] Most experimental work has been performed on paramagnetic materials and superparamagnetic small particles. The observation of relaxation in magnetically ordered compounds has been limited. The effect has been found mainly in materials where one or more magnetic sublattices have been diluted by diamagnetic ions, for instance the Zn and Sn substituted ferrites.[15-18] As a result of the substitution, the magnetic sublattice becomes incomplete. A similar situation occurs for the $FeTiRO_5$ compounds. Here paramagnetic $Fe^{3+}$ and diamagnetic $Ti^{4+}$ ions are equally distributed over $4f$ and $4h$ sites in a random manner. An $Fe^{3+}$ ion at a $4f$ site has four $4h$ and two $4f$ nearest neighbors, whereas a $Fe^{3+}$ at a $4h$ site has four $4f$ and one $4h$ neighbors. Not all neighbors participate in an antiferromagnetic superexchange bond however.[1] Since the distribution of cations is random, the exchange interaction felt by the $Fe^{3+}$ ions varies, and on the average, is not very strong.

It has been suggested by Van der Woude and Dekker[12] that relaxation effects in compounds with incomplete magnetic sublattices may occur at relatively low values of $T/T_N$. At temperatures not much above 0 K the shape of the spectrum is determined by the spin-wave frequency $\omega_s$, which is much higher than the Larmor frequency $\omega_L$. As a result the Zeeman splitting of the ME spectrum is determined by $\langle S_z \rangle$, and consequently $H_{hf}$ should show the same temperature dependence as the sublattice magnetization. At higher temperatures the density of spin-waves increases and eventually the collective behavior of the spin system disap-

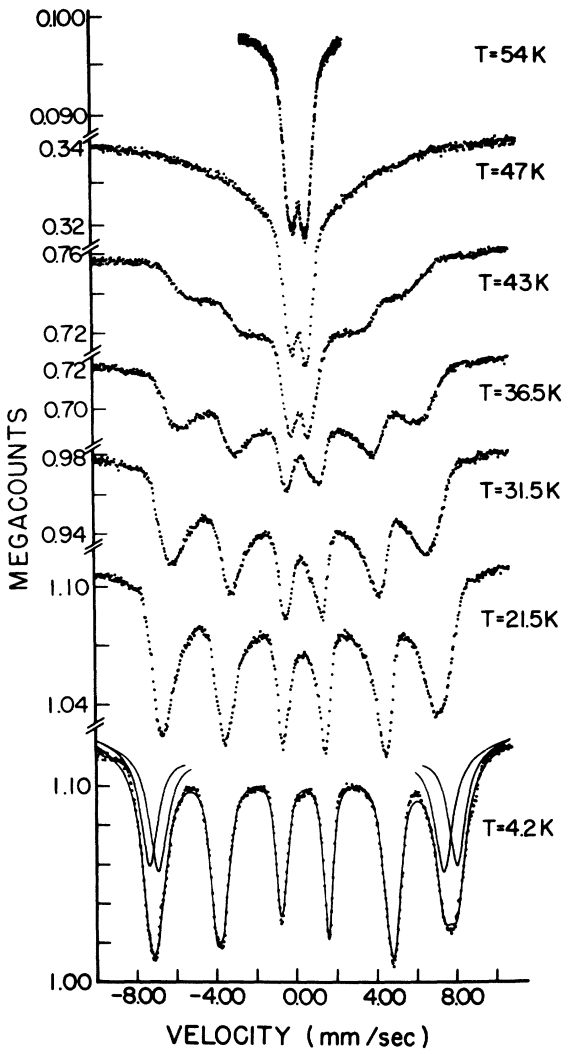


FIG. 5. Mössbauer spectra of $FeTiSmO_5$ as a function of temperature. The Néel temperature for this compound is 52.8 K.

pears. In materials with incomplete magnetic lattices this behavior can occur at rather low values of $T/T_N$. The spin-wave model can then be replaced by a Weiss molecular-field model, which considers a single spin in the average field produced by its neighbors. Then the shape of the spectrum is determined by the ionic spin-flip frequency $\omega_i$ instead of the spin-wave frequency $\omega_s$. For $\omega_i \approx \omega_L$ relaxation effects occur and the hyperfine splitting is no longer proportional to $\langle S_z \rangle$ (see Fig. 6). Since spin-spin relaxation determines the relaxation process in these ordered compounds and the spins are inhomogeneously distributed, various relaxation times for $Fe^{3+}$ ionic spins can be expected in these compounds. The increase of the intensities of the superparamagnetic component between $T/T_N = 0.7$ and 1 can also be understood with a cluster model, as proposed recently by Basile and Poix.[18]

Another consequence of the relaxation effects is that the values of $T_N$ as measured by the ME technique and neutron diffraction or static magnetization measurements are not necessarily the same. Large differences have been reported for some of the ferrites,[17,18] and therefore also can be expected for the $FeTiRO_5$ system.

From susceptibility measurements on single-crystal $FeTiNdO_5$ a transition temperature $T_N \approx 18.6$ K has been determined.[19] With the ME technique a much higher value, $T_N = 33.5$ K, has been found. Now a ME spectrum will show a (broadened) Zeeman-split component as long as there are $Fe^{3+}$ ions with relaxation times comparable to the Larmor precession times even if $\langle S_z \rangle$ has no preferred direction. This mechanism, if acting, would yield a Néel temperature higher than that obtained by magnetization measurements. Another possibility is that the $Fe^{3+}$ and $Ti^{4+}$ cation distributions over the $4f$ and $4h$ sites were different because the thermal treatments employed to make the single-crystal and polycrystalline materials were not the same. A different cation distribution would probably also lead to different Néel temperatures.

For $Mn_{0.95}Fe_{0.05}TiRO_5$ at 4.2 K ($T/T_N = 0.23$) relaxation effects start to become observable. Indeed, for the unsubstituted $MnTiRO_5$ compounds, no magnetic order was detected in neutron-diffraction measurements at 1.5 K.[1] Although the presence of $Fe^{3+}$ ions in $Mn_{0.95}Fe_{0.05}TiNdO_5$ could lead to a magnetic hyperfine-field splitting up to 16 K, it seems more likely that slow relaxation is responsible for this large difference in $T_N$.

For the $Cr_{0.95}Fe_{0.95}TiRO_5$ series, relaxation effects leading to an elevation in the Néel temperature as determined by the Mössbauer effect seem less important. However, relaxation may be partially responsible for the difference between $T_N = 17$ K for $Cr_{0.95}Fe_{0.05}TiNdO_5$, determined by

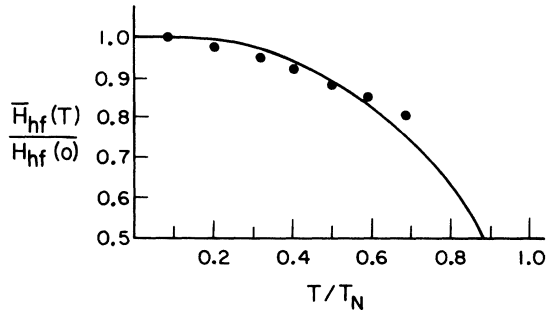


FIG. 6. Experimental temperature dependence of the average reduced hyperfine field compared to the Brillouin curve calculated for $S = \frac{5}{2}$.

the Mössbauer effect, and $T_N = 13$ K for CrTiNdO$_5$, determined by neutron diffraction.

## IV. SUMMARY

The series of $A$Ti$R$O$_5$ compounds ($A$ = Cr, Mn, Fe and $R$ = Pr, Nd, Sm, Eu, Gd) have been investigated using the Mössbauer-effect technique. The results show that the distribution of $A^{3+}$ and $Ti^{4+}$ over square-pyramidal and octahedral sites is not significantly influenced by the rare-earth ion. For the FeTi$R$O$_5$ series, the values of $\epsilon$, $\delta$, $H_{hf}$, and $T_N$ change slightly going from Pr to Gd. Similar but less significant changes have been observed for the $Mn_{0.95}Fe_{0.05}$Ti$R$O$_5$ series. These results are related to the decrease in the dimensions of the unit cell.

At temperatures above 4.2 K, the spectra show relaxation features at values of $T/T_N \ll 1$. A random distribution of the magnetic $A^{3+}$ and the diamagnetic $Ti^{4+}$ cations, which leads to incomplete magnetic sublattices, is suggested as the origin of the relaxation.

## ACKNOWLEDGMENT

This research was financially supported by the National Research Council of Canada.

[1]G. Buisson, J. Phys. Chem. Solids 31, 1171 (1971).
[2]P. J. Schurer and A. H. Morrish, Physica (Utr.) 86-88B, 925 (1977).
[3]G. A. Sawatzky and F. van der Woude, J. Phys. (Paris) Suppl. 35-C6, 47 (1974).
[4]R. P. Gupta and S. K. Sen, Phys. Rev. A 8, 1169 (1973).
[5]J. Owen and D. R. Taylor, Phys. Rev. Lett. 10, 1164 (1966).
[6]N. L. Huang, R. Orbach, and E. Simanek, Phys. Rev. Lett. 17, 134 (1966).
[7]F. van der Woude and G. A. Sawatzky, Phys. Rev. B 4, 3159 (1971).
[8]F. van der Woude and G. A. Sawatzky, *Proceedings of the Conference on Mössbauer Spectrometry* (Phys. Soc. DDR, Dresden, 1971), p. 238; G. A. Sawatzky, C. Boekema, and F. van der Woude, *ibid.*, p. 335.
[9]C. Boekema, F. van der Woude, and G. A. Sawatzky, Int. J. Magn. 3, 341 (1971).
[10]F. Basolo and R. G. Pearson, *Mechanisms of Inorganic Reaction* (Wiley, New York, 1958), p. 55.
[11]A. M. Afanas'ev and Yu Kagan, Zh. Eksp. Teor. Fiz. 45, 1660 (1963) [Sov. Phys.-JETP 18, 1139 (1964)].
[12]F. van der Woude and A. J. Dekker, Phys. Status Solidi 9, 775 (1965).
[13]H. Wegener, Z. Phys. 186, 498 (1965).
[14]M. Blume and Z. A. Tjon, Phys. Rev. 165, 165 (1968).
[15]P. Raj and S. K. Kulshreshta, Phys. Status Solidi A 4, 501 (1971).
[16]S. C. Bhargava and P. K. Iyengar, Phys. Status Solidi B 53, 359 (1972).
[17]C. M. Srivastava, S. N. Shringi, and R. G. Srivastava, Phys. Rev. B 14, 2041 (1976).
[18]F. Basile and P. Poix, Phys. Status Solidi A 35, 153 (1976).
[19]I. Yaeger (private communication).